

## Phase transition, electronic and optical properties of NaCl under pressure

Naemullah

*Department of Physics, G. D. C. Darra Adam Khel, F. R. Kohat, KPK, Pakistan*

G. Murtaza\*

*Materials Modeling Laboratory, Department of Physics,  
Islamia College University, Peshawar, Pakistan  
murtaza@icp.edu.pk*

R. Khenata

*LPQ3M Laboratory, Institute of Science and Technology,  
University of Mascara, Algeria*

Z. A. Alahmed

*Department of Physics and Astronomy, King Saud University,  
Riyadh 11451, Saudi Arabia*

A. H. Reshak

*New Technologies – Research Center, University of West Bohemia,  
Univerzitetni 8, 306 14 Pilsen, Czech Republic  
Center of Excellence Geopolymer and Green Technology,  
School of Material Engineering,  
University Malaysia Perlis, 01007 Kangar, Perlis, Malaysia*

Received 26 August 2013

Revised 18 February 2014

Accepted 19 February 2014

Published 12 March 2014

In this paper, we have carried out a theoretical investigation on the structural and optoelectronic properties of NaCl under pressure effect via first principle calculations within the density functional theory. The structural phase transition from NaCl(B1) to CsCl(B2)-type structures is determined. The compound has a very wide bandgap in both phases. Optical properties including the absorption coefficient, optical conductivity and frequency dependent reflectivity are explained to characterize the optical nature of NaCl up to pressure of 134 GPa.

*Keywords:* NaCl; DFT; pressure effect; optoelectronics; band structure.

\*Corresponding author.

## 1. Introduction

Sodium chloride (NaCl) is known as a prototype for ionic materials. It is used in soda ash, food, medicine and agricultural industry.<sup>1–4</sup> NaCl is a highly compressible solid generally used for pressure calibration. It is also used in diamond anvil cells for thermal insulation as well as pressure transmitting medium. Based on these properties the study of NaCl under pressure is of extra importance. The structural phase transition of sodium chloride under pressure has been reported by several scientists, and they found that this compound undergoes first order phase transition from the six-fold coordinated NaCl-type (B1) structure to the eight-fold coordinated CsCl-type (B2) structure at about 30 GPa.<sup>5–14</sup> Structural properties of NaCl and its equation of state for the upper limit of its pressure up to 30 GPa are examined in Refs. 10–18. Sodium chloride in its B2 phase is also well studied in the range 30–70 GPa in Refs. 7, 11, 19 and 20. Ono *et al.*<sup>21</sup> also reported the structural phase transition from B1 to B2 phase in sodium chloride at 30 GPa and inspected the structural data up to 134 GPa with maintaining B2 phase. However, to the best of our knowledge no theoretical prediction has been reported on the structural and optoelectronic properties of NaCl under pressure up to 134 GPa.

In this paper, we have performed calculations using all electrons full potential linearized augmented plane wave with the mixed basis FP-LAPW+lo method<sup>22,23</sup> as implemented in the WIEN2K computer package<sup>24</sup> to investigate the structural phase transition from B1 to B2 phase, electronic possessions and optical response of the NaCl up to 134 GPa. This work can overcome the lack of data on the optical and electronic properties with and without pressure and to provide important unseen properties of NaCl for further examination.

## 2. Computational Details

The exchange-correlation effects are treated with the generalized gradient approximation of Wu–Cohen<sup>25</sup> and modified Becke–Johnson (mBJ).<sup>26</sup> The calculations were performed with  $R_{\text{MT}} * K_{\text{max}} = 7$  ( $R_{\text{MT}}$  is the smallest muffin–tin radius and  $K_{\text{max}}$  is the cut-off for the plane wave). The muffin–tin sphere radii  $R_{\text{MT}}$  for both Na and Cl were chosen to be 2.5 atomic units (a.u.). To provide a reliable Brillouin zone integration and to get better optical response a set of 2000  $k$ -points in the irreducible wedge of the Brillouin zone was used. The valence wave functions inside the spheres are expanded up to  $l_{\text{max}} = 9$ , while the charge density was Fourier expanded up to  $G_{\text{max}}$  (magnitude of largest vector) = 14 (Ry)<sup>1/2</sup>. The self-consistent calculations are considered to be converged when the total energy of the system is stable within  $10^{-5}$  Ry.

## 3. Results and Discussions

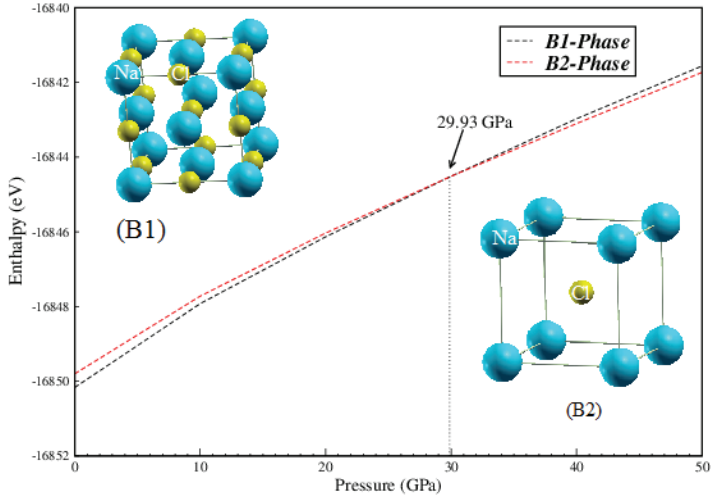
The ground state structural properties of sodium chloride are predicted by calculation of the unit cell energy as a function of unit cell volume in both B1 and B2

phases. Ground state energy of B1 phase is lower than that of B2 phase, indicating that the B1 phase is more stable than the B2 phase at ambient conditions. The evaluation of the zero Kelvin phase transition between the B1 and B2 structures of NaCl can be observed from the usual condition of equal enthalpies, where at certain pressure enthalpy ( $H = U + PV$ ) of both phases is the same. Enthalpies of NaCl are calculated in B1 and B2 phases as a function of pressure from 0 GPa to 60 GPa and shown in Fig. 1(a). Enthalpy difference of the two phases is also plotted as a function of pressure and depicted in Fig. 1(b). Thermodynamically, the phase transition takes place at pressure where the enthalpies of the two phases are equal, and in our case, phase boundary was found to be at 29.93 GPa as shown in Figs. 1(a) and 1(b). The structural phase transition leads to reduce the unit cell volume and consequently increases the coordination from six-fold to eight-fold. Our calculated value of 29.93 GPa for pressure transition from B1 to B2 phase is in excellent agreement with the available experimental and theoretical value of 30 GPa.<sup>5–14,21</sup>

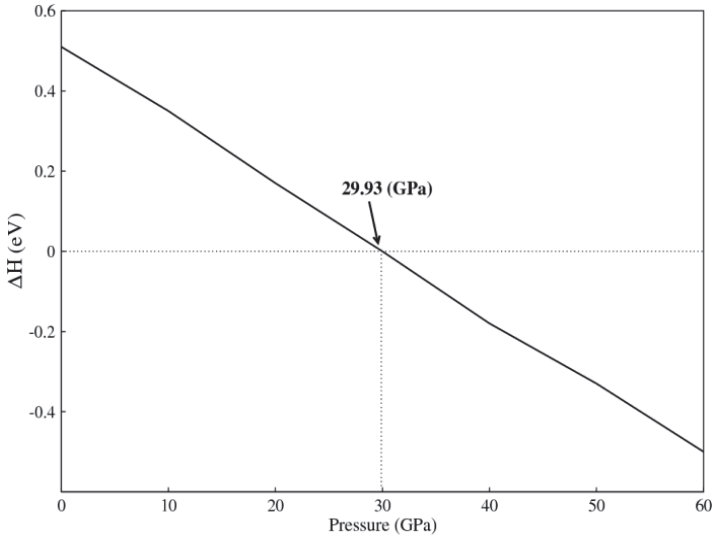
The electronic band structure and density of states under pressure are carried out to explore the electronic properties of sodium chloride. The calculated band structures along high-symmetry lines in the Brillouin zone for B1 at zero pressure and B2 at 30 GPa are shown in Fig. 2. At zero pressure, a direct bandgap of 8.82 eV is found at the  $\Gamma$ -point for B1 phase. The structural phase transition from B1 to B2 at 30 GPa modifies the band structure where a direct bandgap of 7.57 eV is found at the M-point. A decrease in bandgap value is observed when the pressure is applied with no major changes in the band structure in B2 phase.

The electronic densities of states (DOS) of NaCl at different pressures are depicted in Fig. 3. Zero pressure DOS for B1 phase shows that just below the Fermi level, the valence band is formed by Cl-3*p* state with small contribution from Na-2*p* state. Below the valence band, a sharp band situated at around  $\sim 12.5$  eV is observed which is mainly formed by Cl-3*s* state. Above the Fermi level, the conduction band is formed by Na-2*s* with mixed contribution from Cl-3*d*, Na-2*s*, Na-2*p*, Cl-3*s* and Cl-3*p* states. At 30 GPa where the structural phase transition from B1 to B2 phase takes place, the DOS showed an additional band localized at 22 eV below the Fermi level. This band consists mainly of Na-2*p* state. Cl-3*p* state dominates the valence band while conduction band consists of Cl-3*d* state with small contribution from Na-2*p* and Cl-3*s*, 3*p* states. When the pressure increased up to 134 GPa, valence band broadens 75% as compared to 0 GPa valence band. The conduction band contracts with the increase of pressure in the B2 phase. Similar trend has been found for the CsCl which is isoelectronic to NaCl.<sup>27</sup>

The frequency dependant optical properties of NaCl under high pressure from 0 GPa to 134 GPa are described here. Optical absorption behavior of a material can be visualized by its absorption coefficient,  $\alpha(\omega)$ . Frequency dependant absorption coefficient of NaCl at various pressures is shown in Fig. 4. The absorption threshold of NaCl at zero pressure in B1 phase starts at about 9 eV. The threshold occurs due to the interband transitions of electrons from the top of the valence band to



(a)



(b)

Fig. 1. (Color online) (a) Variation of enthalpies per formula units as a function of pressure for NaCl compounds in both structures, B1 and B2. The arrow marks the calculated transition pressure  $P_t$ . The crystal structure of NaCl in B1 and B2 phases are inside. (b) The enthalpy difference between B1 and B2 phases versus pressure. The arrow marks the calculated transition pressure  $P_t$ .

the bottom of the conduction band. At zero pressure, one distinctive high peak at 13.5 eV appears due to the transition of electrons from the Cl-3*p* state in valence band to the unoccupied Na-3*s*, 3*p* and Cl-3*d* states in the conduction band. A phase transition from B1 to B2 at 30 GPa produces the high multiplex behavior instead

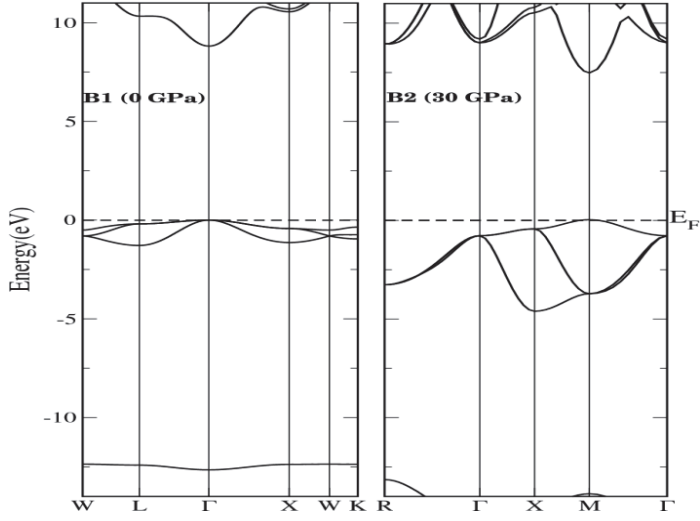


Fig. 2. Band structure along high symmetry directions of NaCl in B1 and B2 phases.

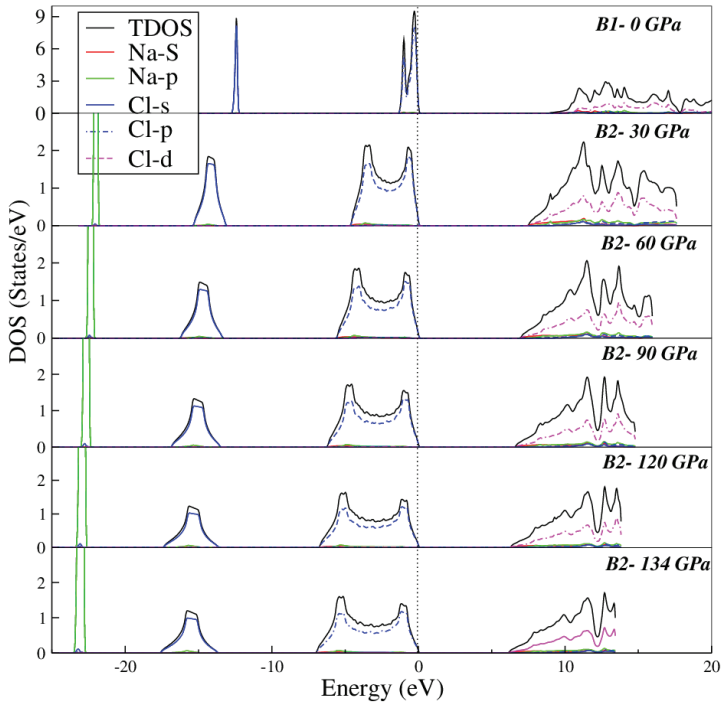


Fig. 3. (Color online) Total and partial density of states of NaCl at various pressures.

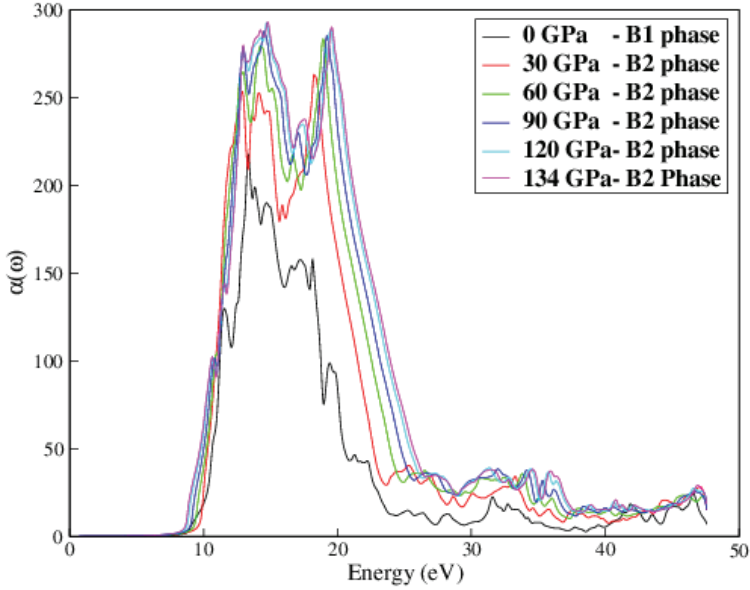


Fig. 4. (Color online) Absorption coefficient of NaCl as a function of energy at various pressures.

of single peak at zero pressure. Absorption peaks at 12.8 eV and 15 eV are due to interband transitions to the unoccupied Cl-3d state of the conduction band from the Cl-3p state of valence band. Another peak at 18 eV is also due to the electron transitions from occupied Cl-3p state in the bottom of the valence band to the Cl-3d state of the conduction band.

Optical conductivity of NaCl at various pressures is depicted in Fig. 5. At zero pressure and in B1 phase, the optical conductivity threshold starts about 9 eV and attains the maximum value of  $9.2 \times 10^3 \Omega^{-1} \text{ cm}^{-1}$ . At 30 GPa, due to a structural phase transition from B1 to B2 the maximum optical conductivity increases to  $1.3 \times 10^4 \Omega^{-1} \text{ cm}^{-1}$  and shifts toward lower energy. By increasing pressure to 60 GPa, a high peak progresses toward higher energies. Same trend can be seen up to high pressure of 134 GPa. The increase in pressure increases the maximum optical conductivity which is  $1.7 \times 10^4 \Omega^{-1} \text{ cm}^{-1}$  at 134 GPa, and the threshold point moves toward lower energies while maximum peaks shift to higher energies.

The frequency dependant reflectivity,  $R(\omega)$ , in pressure range of 0–134 GPa is shown in Fig. 6. At 0 GPa, zero frequency reflectivity  $R(0)$  is 4% which increases to 8% at 134 GPa. The highest peak of reflectivity at zero pressure is 40% and reaches to 70% at 134 GPa. Applications of high pressure make the material more reflecting which is due to the decrease in the bandgap of the material under pressure. These high peaks shift toward higher energies with an increase in pressure. High reflectivity range of 11.43–21 eV at zero pressure broadened over 10–24 eV at 134 GPa.

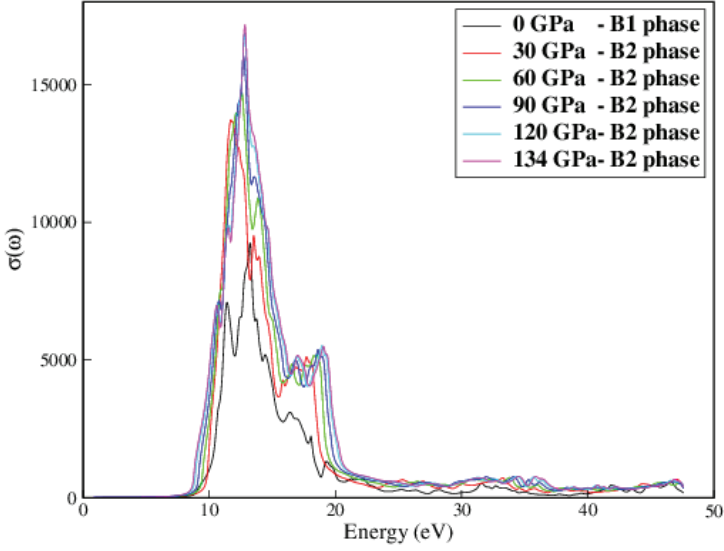


Fig. 5. (Color online) Optical conductivity of NaCl as a function of energy at various pressures.

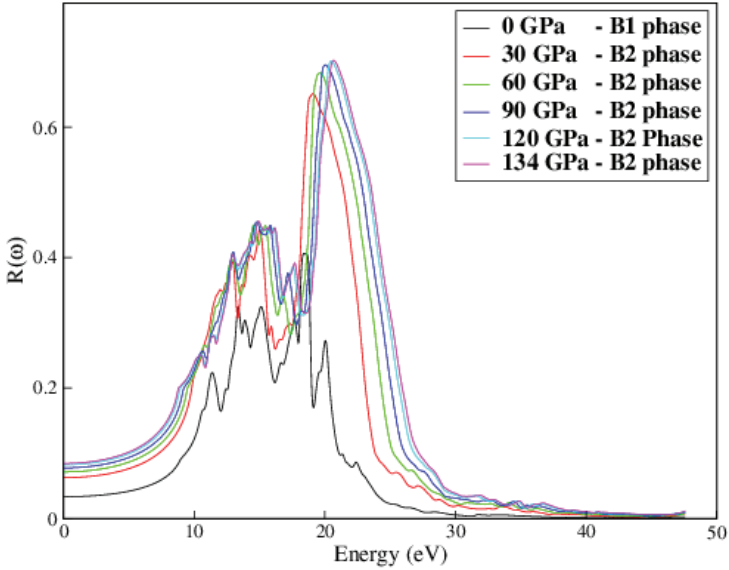


Fig. 6. (Color online) Frequency dependant reflectivity of NaCl as a function of energy at various pressures.

#### 4. Conclusion

Phase transition and optoelectronic properties of NaCl have been computed through the FP-LAPW method using GGA and mBJ exchange and correlation potentials. It is predicted that at a pressure of 29.93 GPa, the phase transition takes place

from B1 to B2 structure which is in excellent agreement to the experimental value of 30 GPa. Energy bandgaps are found to be wide and direct in both B1 and B2 phases. Bandgap value decreases by increasing the pressure in both phases. The energy bands in B2 phase are wider compared to those in B1 phase. From the optical spectra, a high absorption is observed in the ultraviolet region, and the material is transparent in both structural phases. The maximum absorption coefficient, optical conductivity and reflectivity increase with the increase in pressure.

### Acknowledgment

For author A. H. Reshak, the result was developed within the CENTEM project, Reg. no. CZ.1.05/2.1.00/03.0088, co-funded by the ERDF as part of the Ministry of Education, Youth and Sports OP RDI programme. Author R. Khenata acknowledges the financial support provided by the Deanship of Scientific Research at King Saud University for funding the work through the research group project No. RPG-VPP-088.

### References

1. M. D. Kiefer, *Today's Chemist at Work* **11** (2002) 87–88.
2. E. R. Riegel, *Riegel's Handbook of Industrial Chemistry* (2003), p. 436.
3. G. Westphal, G. Kristen, W. Wegener, P. Ambatiello, H. Geyer, B. Epron, C. Bonal, G. Steinhauser and F. Götzfried, *Ullmann's Encyclopedia of Industrial Chemistry* (Wiley-VCH, Weinheim, 2002).
4. D. S. Kostick, *Salt*, U.S. Geological Survey Minerals Yearbook (USGS, 2008).
5. W. A. Bassett, T. Takahashi, H. K. Mao and J. S. Weaver, *J. Appl. Phys.* **39** (1968) 319–325.
6. L. Liu and W. A. Bassett, *J. Appl. Phys.* **44** (1973) 1475–1479.
7. Y. Sato-Sorensen, *J. Geophys. Res.* **88** (1983) 3543–3548.
8. S. Froyen and M. L. Cohen, *J. Phys. C* **19** (1986) 2623–2632.
9. X. Li and R. Jeanloz, *Phys. Rev. B* **36** (1987) 474–479.
10. E. Apra, M. Causa, M. Prencipe, R. Dovesi and V. R. Saunders, *J. Phys.: Condens. Matter* **5** (1993) 2969–2976.
11. A. M. Hofmeister, *Phys. Rev. B* **56** (1997) 5835–5855.
12. C. S. Sims, G. D. Barrera, N. L. Allan and W. C. Mackrodt, *Phys. Rev. B* **57** (1998) 11164–11172.
13. N. Nishiyama, T. Katsura, K. Funakoshi, A. Kubo, T. Kubo, Y. Tange, Y. Sueda and S. Yokoshi, *Phys. Rev. B* **68** (2003) 134109.
14. N. Kana, S. Khamlich, J. B. K. Kana and M. Maaza, *Surf. Rev. Lett.* **20** (2013) 1350001.
15. D. L. Decker, *J. Appl. Phys.* **42** (1971) 3239–3244.
16. J. M. Brown, *J. Appl. Phys.* **86** (1999) 5801–5808.
17. D. L. Decker, *J. Appl. Phys.* **36** (1965) 157–161.
18. E. A. Perez-Albuerne and H. G. Drickmer, *J. Chem. Phys.* **43** (1965) 1381–1387.
19. D. L. Heinz and R. Jeanloz, *Phys. Rev. B* **30** (1984) 6045–6049.
20. N. Sato, G. Shen, M. L. Rivers and S. R. Sutton, *Phys. Rev. B* **65** (2002) 104114.
21. S. Ono, T. Kikegawa and Y. Ohishi, *Solid State Commun.* **137** (2006) 517–521.
22. K. M. Wong, S. M. Alay-e-Abbas, Y. Fang, A. Shaukat and Y. Lei, *J. Appl. Phys.* **114** (2013) 034901.



23. K. M. Wong, S. M. Alay-e-Abbas, A. Shaukat, Y. Fang and Y. Lei, *J. Appl. Phys.* **113** (2013) 014304.
24. P. Blaha, K. Schwarz, G. H. K. Madsen, D. Kvasnicka and J. Luitz, *WIEN2k: An Augmented Plane Wave Plus Local Orbitals Program for Calculating Crystal Properties* (Vienna University of Technology, Austria, 2001).
25. Z. Wu and E. R. Cohen, *Phys. Rev. B* **73** (2006) 235116.
26. F. Tran and P. Blaha, *Phys. Rev. Lett.* **102** (2009) 226401.
27. Naeemullah, G. Murtaza, R. Khenata, A. H. Reshak, S. Naeem and M. N. Khalid, *Int. J. Mod. Phys. B* **28** (2014) 1450047.